

Enhancing the Series Cascade Control Architecture to Regulate Non-minimum Phase Systems

Navlesh Kumar¹, Prashant Garg², Ravindra Singh Kushwah³

Vikrant Institute of Technology and Management, Gwalior, India^{1,2,3}

Abstract: The paper works propose that uses a decomposed outer loop of a series cascade scheme to weave together a fractional Internal Model regulate (IMC) filter, inverse response, and dead-time compensator to regulate the non-minimum phase system. The outer loop process model is divided into two sections due to its higher-order nature. We call this process decomposition. For the inner loop and the first segment of the outer loop that has broken down, the traditional IMC controller is used. After the fractional filter, inverse response, and dead-time compensator in the IMC framework are held accountable, the controller setting for a further decomposed portion of the outer loop is obtained. The benefits of this recommended method are starting to outweigh those of the current control systems. The system's stability is assessed using the Riemann sheet principle. In addition, a robustness test is conducted using sensitivity analysis to look at the effectiveness of the suggested controller. The value of the suggested controller is illustrated by two case studies

Keywords: Proportional integral derivative controller (PID), Internal Model Control (IMC), Fractional Order Controllers (FOC), Integer Order Controllers (IOC), Fractional PID, Cascade control, Stability analysis, Robustness analysis

I. INTRODUCTION

Cascade control performs more effectively than a single loop feedback control. Therefore, the dynamics and actuator nonlinearities cascade structure with flow and pressure loops are utilized in the sluggish processes. The inner and outer loops constitute cascade control. The negative impact of the inner loop influences the outer loop's input in cascade control. In a cascade control scheme, the outer loop monitors the setpoint while the inner loop rejects the disturbances. There are two classifications for cascade controls: series and parallel. Through the use of a controlled variable, cascade regulates the outer loop outcomes in a series [1, 2] recommended to improve the cascade control system. Better cascade control is provided, based on the outer loop decomposition methodology [3]. The unstable system's enhanced cascade control is discussed [4]. Additionally, a proportional integral–proportional–derivative is proposed [5] for process integration within a framework of a single feedback loop. To build the controller in a cascade architecture for combining unstable and stable processes, a combination arrangement is addressed [6]. In process industries, however, a nonminimum phase (NMP) zeros method is ubiquitous. On the other hand, certain approaches demonstrate their first impact with respect to zero frequency gain in process industries. They define it as an NMP system. Open loop zeros in the plant transfer function are the source of the state-of-the-art for the inverse response. It integrates limits on the robustness of the closed-loop system and shows how gain margin is restricted [7]. Surprisingly a reformatory signal is produced by an inverse response compensator as the inverse response characteristic decreases. For NMP systems, the proportional-integral-derivative (PID) controller is automatically utilized [8]. The PID controller's universality extends to fractional order and is not limited to integer order. A PID controller based on fractional filters has been used recently [9]. Postponed There was discussion of Bode's ideal transfer function methodology with fractional order controller [10]. In addition, [11] describes the cascade fractional PI controller. However, the improved cascade control performance is due to the tuning strategy. One typical tuning technique is Internal Model Control (IMC) [1]. The fractional filter method based on IMC is used [12]. A fractional IMC filter-based cascade control scheme was proposed [13]. A new IMC technique for tuning cascade control systems is proposed [14]. The genetic algorithm is utilized for cascade control [15]. Based on fractional filters, the IMC series cascade control with optimization technique was originally presented [16].

Primarily, an inverse response compensator and fractional filter combined with a series cascade scheme has been utilized in the IMC environment. However, there is not an obvious method that integrates the derivative controller with the NMP system's outer loop process model. This paper offers an innovative perspective into how an NMP system's feedback derivative controller and outer loop process model are connected. The benefit of this approach is that it exhibits improved performance without compromising robustness. This proposed structure further improves the set point filter prevention. Furthermore, both controllers are IMC for ease of use. Moreover, the stability of the proposed method is evaluated using the Riemann sheet theory.

The NMP mechanism is introduced in the paper's opening paragraph. Preliminaries are presented in Section 2. In Section 3, the proposed work is illustrated. Section 4 has the simulation and Results. Section 5 contains the conclusion.

II. PRELIMINARIES

This section covers the mathematical fundamentals needed to carry out the theoretical development and application of the suggested controller to real-world issues.

Series Cascade Control

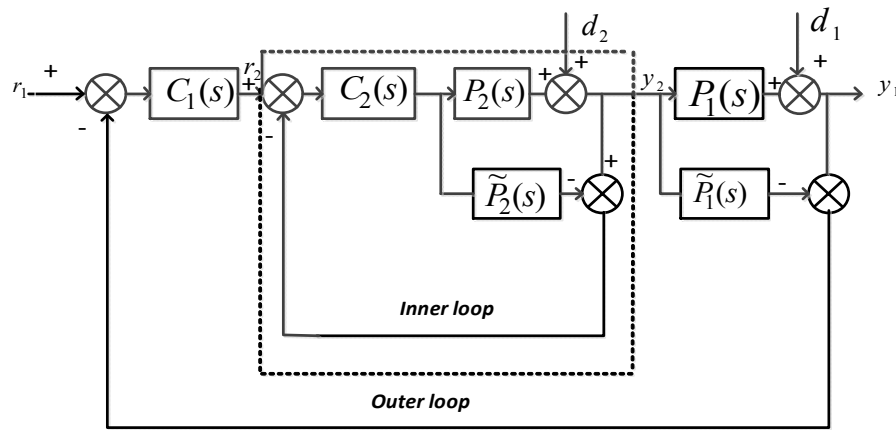


Fig.1 Traditional series cascade scheme

$C_1(s)$, $C_2(s)$ are the outer and inner loop controller shown in Fig. 1, it is also termed as master and slave controller. It comprises are two processes $P_1(s)$, $P_2(s)$ with their process model $\tilde{P}_1(s)$ and $\tilde{P}_2(s)$. Here r_1 , y_1 , d_1 and r_2 , y_2 , d_2 are the input, output and disturbances of inner and outer loop. The transfer function of both loops can be determined easily which can be written as [7]

$$\begin{aligned} y_2(s) &= P_2(s)C_2(s)r_2 + (1 - P_2(s)C_2(s))d_2. \\ y_1(s) &= P_2(s)C_2(s)P_1(s)C_1(s)r_1 + (1 - P_2(s)C_2(s)) \\ &\quad (1 - P_2(s)C_2(s)P_1(s)C_1(s))d_2 + ((1 - P_2(s)C_2(s)P_1(s)C_2(s))d_1. \end{aligned}$$

III. PROPOSED WORK

Proposed series cascade control scheme: Section II (A) discusses the traditional series cascade control scheme. However, it loses out on excellent closed-loop performance if there is a lot of dead time and NMP zeros in the outer loop. The proposed control scheme is shown in Fig. 2. The deconstructed outer loop is used to weave together the higher order fractional filter, inverse response compensator, and dead-time compensator in that system.

$$\begin{aligned} y_1(s) &= P_2(s)C_2(s)P_1(s)\{C_1(s)I(s)\}r_1(s) + (1 - P_2(s)C_2(s)) \\ &\quad (1 - P_2(s)C_2(s)P_1(s)\{C_1(s)I(s)\}d_2 + ((1 - P_2(s)C_2(s)P_1(s)C_1(s)I(s))d_1. \end{aligned}$$

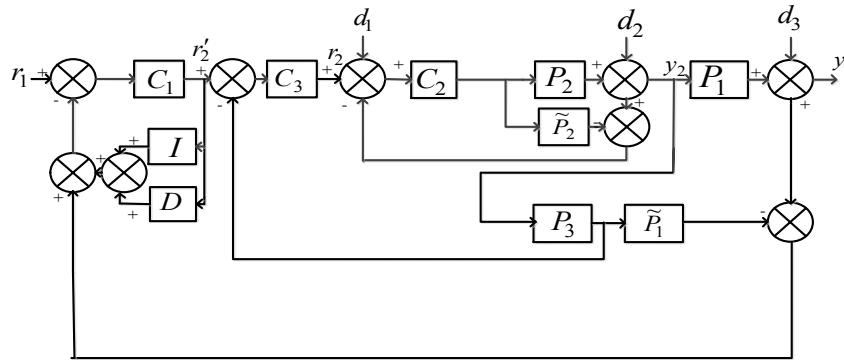


Fig. 2 Proposed series cascade scheme

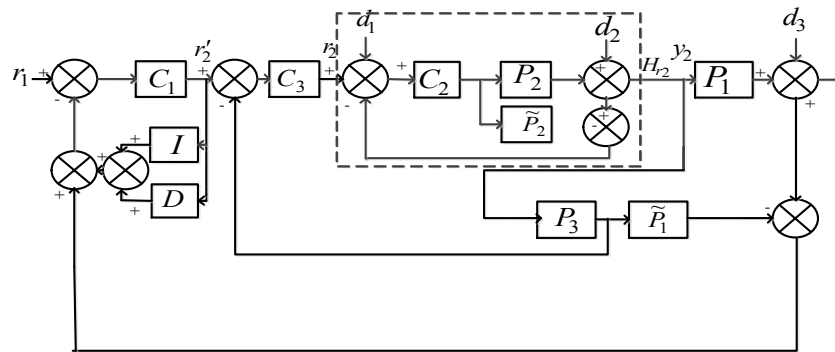


Fig. 3 Modified version of proposed scheme

In IMC context inner loop controller can be written as [1]

$$C_2(s) = \frac{f(s)}{\tilde{P}_2^-(s)} \quad (3.1)$$

Here $f(s) = \frac{1 - \frac{Ls}{2} + \frac{L^2 s^2}{12}}{1 + \frac{Ls}{2} + \frac{L^2 s^2}{12}}$ is a low pass filter while $\tilde{P}_2^-(s)$ interprets the minimum phase part of the process model. Now from Fig. 2 output of the inner loop becomes,

$$\frac{y_2(s)}{r_2(s)} = H_{r_2}(s) = P_2(s)C_2(s) \quad (3.2)$$

Modified version of proposed scheme is displayed in Fig. 3

$$P_3' = H_{r_2}(s)P_3 \quad (3.3)$$

Now output of the decomposed part of outer loop

$$\frac{y_2(s)}{r_2'(s)} = H_{r_3}(s) = C_3(s)P_3' \quad (3.4)$$

Simplified version of proposed scheme is shown in Fig. 4 In IMC context inner loop controller can be written as [1]

$$C_3(s) = \frac{f_3(s)}{\tilde{P}_3^-(s)} \quad (3.5)$$

Afterward overall plant transfer function transfer function becomes,

$$P(s) = H_{r_3}(s) \frac{P_1(s)}{P_3(s)} \quad (3.6)$$

Now utilize generalized controller transfer function [17]

$$C(s) = \frac{\tilde{P}^+(s)e^{-Ls}}{\tilde{P}(s)e^{-Ls}[f(s)^{-1}\tilde{P}(s) - \tilde{P}^+(s)] - 2bs - \tilde{P}(s)\tilde{P}^+(s)(1 - e^{-Ls})} \quad (3.7)$$

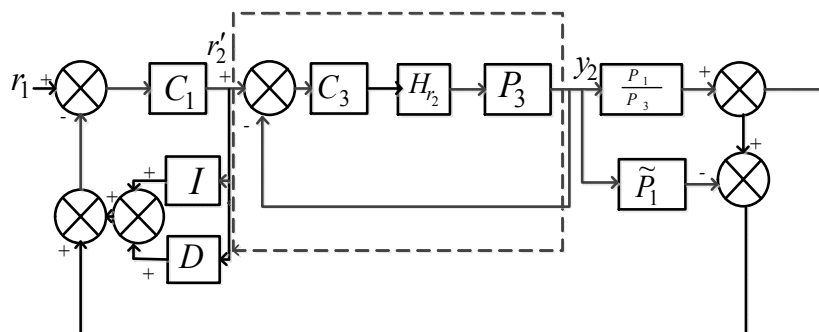


Fig. 4 Simplified version of proposed scheme

Design of C_2 with FOPDT model:

$$P_2(s) = \frac{K_2 e^{-L_2 s}}{(1 + T_2 s)}$$

Here K_2 , L_2 and T_2 shows process gain, delay time and time constant of inner loop. The inner loop IMC filter (Seborg,2004)

$$f_1(s) = \frac{1}{(\lambda_2 s + 1)^r}$$

Where λ_2 is the tuning parameter. r is chosen in such a way to make controller proper. According to IMC concept, the process model is decomposed into two parts minimum phase part $\tilde{P}_2^-(s) = \frac{K_2}{1+T_2s}$ and non-minimum phase part e^{-L_2s} .

After utilization equation (3.1) the inner loop IMC controller becomes

$$C_2(s) = \frac{1 + T_2 s}{K_2(\lambda_2 s + 1)} \quad (3.8)$$

Here λ_2 can be tuned on the basis of maximum sensitivity [19].

$$\lambda_2 = \frac{-0.7289M_s + 1.55}{M_s - 1.006}L_2 \quad (3.9)$$

The outer loop controllers are decomposed into two parts i.e., [18]

$$P_1(s) = \frac{K_1(1-bs)}{s}e^{-L_1s} \text{ and } P_3(s) = \frac{K_3}{s}$$

Design of C_3 with IO (Integer order) model:

$$P_3(s) = \frac{K_3}{s}$$

Since output of the inner loop transfer function acts as a input to the integer order controller. After utilization equation (3.2) the plant transfer function becomes

$$P_3'(s) = \frac{K_3 e^{-L_2 s}}{s(\lambda_2 s + 1)} \quad (3.10)$$

After utilization equation (3.4) the controller transfer function for first decomposed component of outer loop,

$$C_3(s) = \frac{s(\lambda_2 s + 1)}{K_3(\lambda_3 s + 1)} \quad (3.11)$$

Here λ_3 is a tuning parameter which can be tuned by equation (3.8).

After utilization equation (3.3) the output of the first decomposed outer loop becomes

$$H_{r_3}(s) = \frac{e^{-L_2 s}}{\lambda_2 s + 1}$$

After utilization equation (3.5) the overall plant transfer function becomes

$$P(s) = \frac{K_1(1 - bs)e^{-Ls}}{s(\lambda_2 s + 1)} \quad (3.12)$$

Here $L = L_1 + L_2$

After the utilization of equation (3.6), the outer loop controller transfer function with higher-order fractional IMC filter and higher-order time delay approximation becomes,

$$C(s) = \frac{s(\lambda_3 s + 1) \left(1 + \frac{Ls}{2} + \frac{L^2 s^2}{12}\right)}{\lambda^2 s^{2\eta+2} + 2\lambda s^{\eta+1} + \frac{bL^2 \phi s^4}{12} + s^3 \left(\frac{bL\phi}{2} + \frac{bL^2}{12} - \frac{L^2 \phi}{12}\right) + s^2 \left(\frac{bL}{2} - \frac{L^2}{12} - b\phi - \frac{L\phi}{2}\right) - s \left(b + \frac{L}{2} + \phi\right)} \quad (3.13)$$

Subsequently, separate the equation (3.12) into fractional filter and PID controller then it becomes,

$$C(s) = \frac{(\lambda_3 s^2 + s) \left(\frac{L}{2} \left(1 + \frac{1}{Ls/2} + \frac{Ls}{6}\right)\right)}{\lambda^2 s^{2\eta+1} + 2\lambda s^{\eta} + \frac{bL^2 \phi s^3}{12} + s^2 \left(\frac{bL\phi}{2} + \frac{bL^2}{12} - \frac{L^2 \phi}{12}\right) + s \left(\frac{bL}{2} - \frac{L^2}{12} - b\phi - \frac{L\phi}{2}\right) - \left(b + \frac{L}{2} + \phi\right)}$$

Here λ and η are the fractional-filter parameters which can be tuned by Bode's ideal transfer function [17],

$$\lambda = \frac{\pi - PM}{\frac{\pi}{2}} - 1, \quad \eta = \frac{1}{(\omega_{gc})^{\lambda+1}}$$

ϕ is another tuning parameter which can be tuned by [19]

$$\phi = \lambda_2 \left[1 - \sqrt{\left(1 - \frac{\lambda}{\lambda_2}\right)^3 e^{-\frac{L}{\lambda_2}}} \right]$$

Design of $C_2(s)$:

The design of the inner loop controller is the same as the previous case,

$$C_2(s) = \frac{1 + T_2 s}{K_2(\lambda_2 s + 1)}$$

After utilization equation (3.2) output of the inner loop becomes

$$H_{r_2}(s) = \frac{e^{-L_2 s}}{\lambda_2 s + 1}$$

Design of $C_3(s)$:

After utilization equation (3.10) the plant transfer function becomes

$$P'_3(s) = \frac{K_3 e^{-L_2 s}}{(T_3 s + 1)(\lambda_2 s + 1)} \quad (3.14)$$

After utilization equation (3.11) the controller transfer function for first component of outer loop becomes

$$C_3(s) = \frac{s(\lambda_2 s + 1)(T_3 s + 1)}{K_3(\lambda_3 s + 1)} \quad (3.15)$$

After utilization equation (3.6) the overall plant transfer function becomes

$$P(s) = \frac{K_1(1 - bs)e^{-Ls}}{s(\lambda_3 s + 1)(T_1 s + 1)} \quad (3.16)$$

Consequently, controller design in IMC framework is presented previously. After utilization of generalized equation (3.7) for controller design, then it becomes

$$C(s) = \frac{(\lambda_3 s^3 + s^2(T_1 + \lambda_3) + s) \left(\frac{L}{2} \left(1 + \frac{1}{Ls/2} + \frac{Ls}{6}\right)\right)}{\lambda^2 s^{2\eta+1} + 2\lambda s^{\eta} + \frac{bL^2 \phi s^3}{12} + s^2 \left(\frac{bL\phi}{2} + \frac{bL^2}{12} - \frac{L^2 \phi}{12}\right) + s \left(\frac{bL}{2} - \frac{L^2}{12} - b\phi - \frac{L\phi}{2}\right) - \left(b + \frac{L}{2} + \phi\right)} \quad (3.17)$$

IV. SIMULATION AND RESULTS

This section limits the evaluation of the suggested scheme's effectiveness to processes with inverse responses and dead times. Process parameter variations are reversed in case studies with nominal and +10% values. Bode's ideal transfer

function is used to select the fractional filter parameter ϕ and μ . The stability inequality $PM > 2 \arcsin(1/2S_{\max.})$ is used to evaluate the phase margin [20].

Case Study I

A double integrating process transfer function with inverse response plus dead time is considered. Which can be written as [21]

$$P_1(s) = \frac{(1 - 0.7s)e^{-0.1}}{s^2}$$

$$P_2(s) = \frac{e^{-0.1}}{s + 1}$$

After utilization equation (3.8) the inner loop controller transfer function becomes,

$$C_2(s) = \frac{1 + s}{0.4s + 1}$$

Here $\lambda_2 = 0.4$ which can be chosen on maximum sensitivity M_s . After utilization equation (3.10) the plant transfer becomes

$$P'_3(s) = \frac{e^{-0.1s}}{s(0.4s + 1)}$$

After utilization of equation (3.11) the controller transfer function for P'_3 becomes

$$C_3(s) = \frac{s(0.4s + 1)}{0.2s + 1}$$

After that utilization of equation (3.12) the overall plant transfer function becomes,

$$P(s) = \frac{(1 - 0.7s)e^{-0.2s}}{s(s + 1)} \quad (4.1)$$

The recommended controller settings for the outer loop in the fractional IMC framework can be obtained via equation 3.13),

$$C(s) = \frac{s^2 + s}{s^{1.90} + 2s^{0.45} + 0.000067s^3 + 0.0023s^2 - 0.013s - 0.4} \left(0.1 + \frac{2}{s} + 0.3s \right) \quad (4.2)$$

In Fig.5 shows that the proposed control scheme has less magnitude jump in nominal and +10% mismatch with disturbances. Table 1 shows transient response for double integrating process.

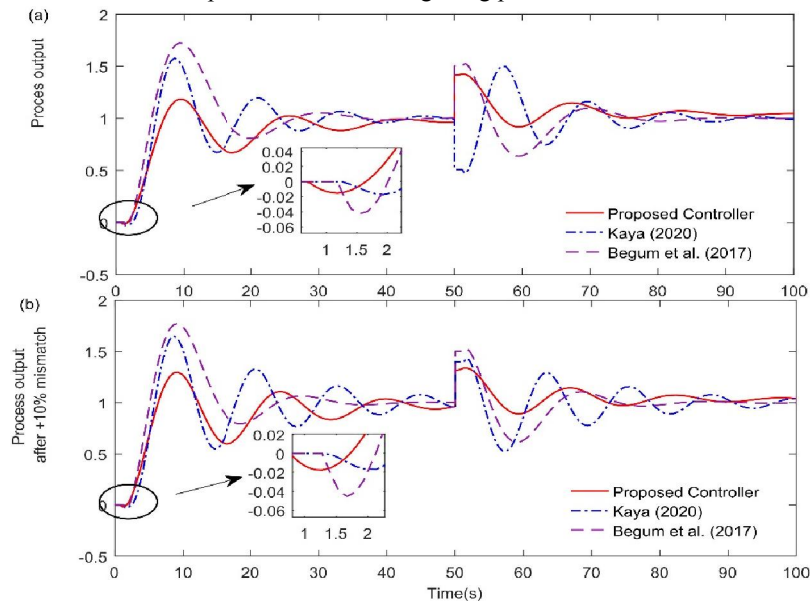


Fig. 5 Comparative study of for double integrating process

Table 1: Transient response for double integrating process

Method	Nominal Case				+10% mismatch case			
	Peak overshoot ratio, %	Rise time, s	IAE	ISE	Peak overshoot ratio, %	Rise time, s	IAE	ISE
Proposed controller	1.18	9.4	0.17	0.0031	1.29	4.6	0.04	0.00
Kaya (2020)	1.53	2.45	0.069	0.027	1.6	3.1	0.13	0.017
Begum et al. (2017)	1.68	2.32	3.4	11.92	1.7	2.2	3.6	13.5

Stability analysis:

The Riemann surface is now crucial to the stability analysis of the proposed structure. The FOMCON toolbox in MATLAB is used to verify the graphical valuation. The stability analysis of the double integer order plus time delay system appears globally as

$$f(s) = 1 + \lambda^2 s^{2\eta+2} + 2\lambda s^{\eta+1} + \frac{bL^2 \varphi s^4}{12} + s^3 \left(\frac{bL\varphi}{2} + \frac{bL^2}{12} - \frac{L^2 \varphi}{12} \right) + s^2 \left(\frac{bL}{2} - \frac{L^2}{12} - b\varphi - \frac{L\varphi}{2} \right) - s \left(b + \frac{L}{2} + \varphi \right)$$

Choose $\alpha = s^\gamma$, Where $s^{0.001} = \alpha$

$$f(s) = 1 + \alpha^{2900} + 2\alpha^{1450} + 0.000067\alpha^{4000} + 0.0023\alpha^{3000} - 0.013\alpha^{2000} - 0.4s^{1000}.$$

Then, instability is revealed by the roots of the natural degree quasi characteristic polynomial inside the Riemann sheet, whereas stability is revealed by the roots outside the Riemann sheet. Every root in Fig. 6 is located outside of the Riemann sheet.

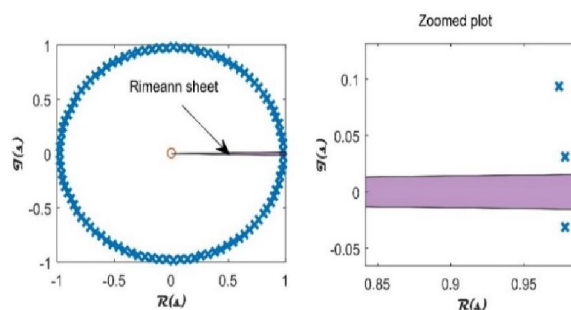


Fig. 6 Stability analysis of double integrating system

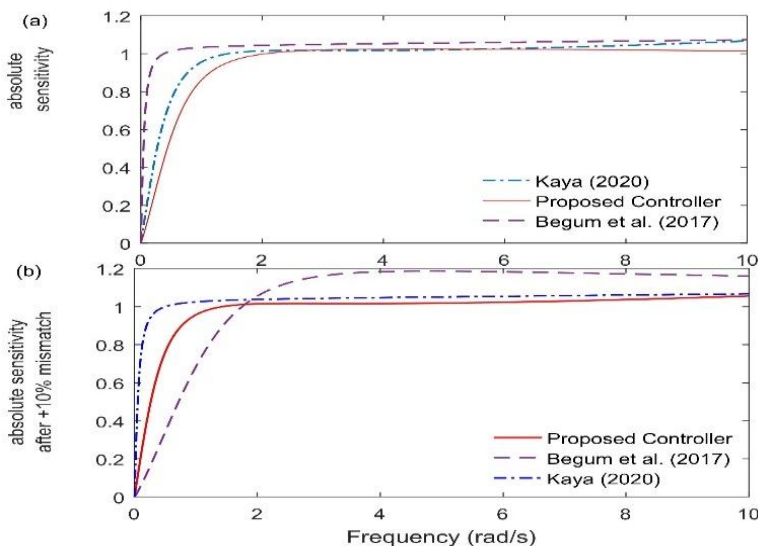


Fig. 7 Robustness analysis of proposed controller for double integrating process

Robustness analysis:

Furthermore, any variation in the dynamics of the process and disturbances can alter the limited description of the feedback system. One way to write the universal sensitivity function is as [20].

$$S(s) = \frac{1}{1 + \bar{P}(s)C(s)} \quad (4.3)$$

Fig. 7 shows the graphical explanation of the suggested controller's robustness analysis. In nominal and 10% model mismatch scenarios, the provided controllers show a reduced increase in maximum sensitivity.

Case study 2

Consider a higher order process transfer function with inverse response and dead-time [21].

$$P_1 = \frac{(1 - 0.5s)e^{-0.4s}}{s(0.5s + 1)(0.4s + 1)} \quad P_2 = \frac{0.5e^{-0.34s}}{(0.1s + 1)}$$

After utilization equation (3.1) the inner loop controller transfer function becomes

$$C_2(s) = \frac{0.1s + 1}{0.5(s + 1)}$$

After that utilization of equation (3.14) the plant transfer function becomes,

$$P'_3(s) = \frac{e^{-0.3s}}{(s + 1)(0.4s + 1)}$$

The controller transfer function is obtained after utilization of equation (3.15),

$$C_3(s) = \frac{(s + 1)(0.4s + 1)}{(0.2s + 1)}$$

Now the output of the first decomposed part of outer loop,

$$H_{r3}(s) = \frac{e^{-0.3s}}{0.2s + 1}$$

After utilization equation (3.16) the overall plant transfer function becomes,

$$P(s) = \frac{(1 - 0.5s)e^{-0.7s}}{s(0.5s + 1)(0.2s + 1)} \quad (4.4)$$

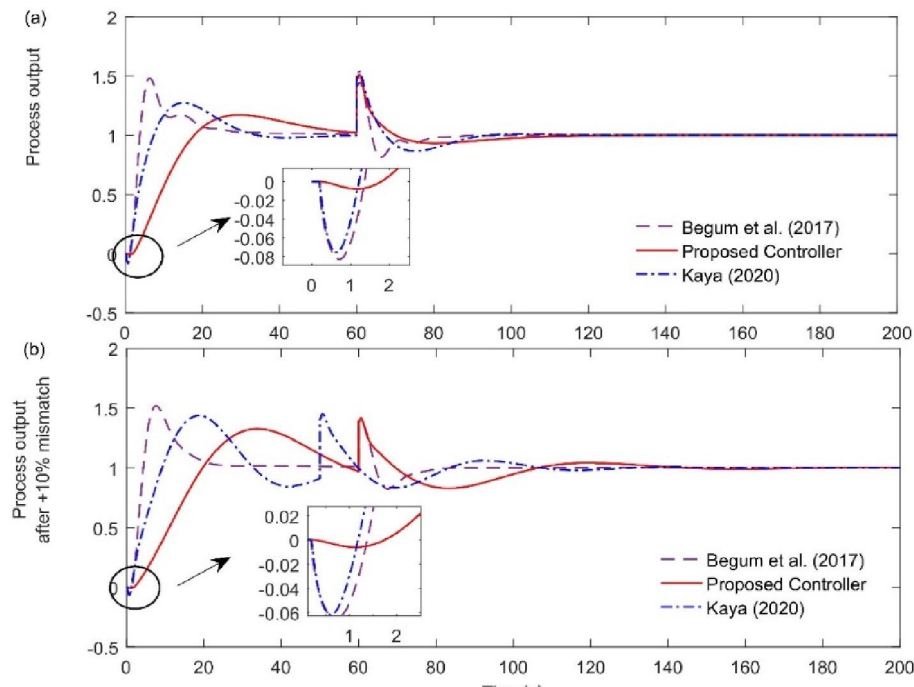


Fig. 8 Relative analysis of proposed controller for higher order process

After utilization of equation (3.17) structure of controller transfer function becomes,

$$C(s) = \frac{0.20s^3 + 0.9s^2 + s}{0.25s^{1.90} + s^{0.45} + 0.0020s^3 + 0.05s^2 + 0.045s - 0.95} \left(0.35 + \frac{0.39}{s} + 0.038s \right) \quad (4.5)$$

Fig. 8 indicates that after +10% mismatch proposed control organisation is verified convincible outcomes in terms of overshoot and undershoot. Table 2 shows transient response for double integrating process.

Method	Nominal Case				+10% mismatch case			
	Peak overshoot ratio, %	Rise time,s	IAE	ISE	Peak overshoot ratio, %	Rise time, s	IAE	ISE
Proposed controller	1.17	14.3	1.3	1.7	1.32	33	3.4	11.72
Kaya (2020)	1.27	10.7	0.16	0.027	1.43	17	0.76	0.58
Begum et al. (2017)	1.4	2.3	0.651	0.42	1.5	7.5	2.5	6.25

Table 2: Transient response and performance indices for higher order integrating process

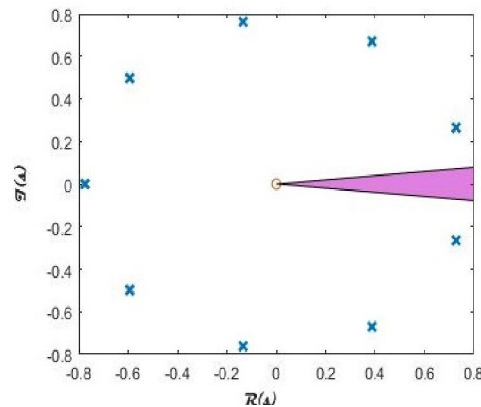


Fig. 9 Stability analysis of higher order process

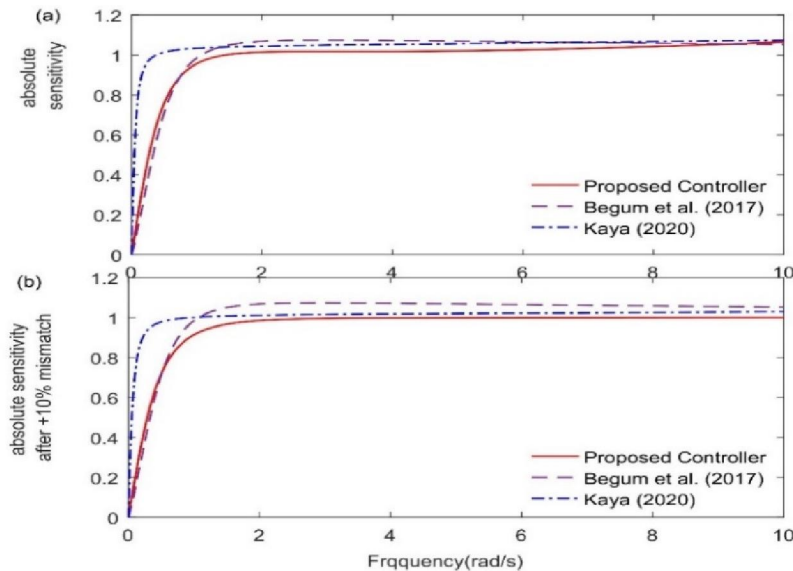


Fig. 10 Robustness analysis of proposed controller for higher order process

Stability analysis:

The detailed description of stability analysis is presented in case study 1. Likewise, the specific arrangement of the fractional characteristic polynomial related to the closed-loop of higher order integrating process is demonstrated

$$f(s) = 1 + s^{2.90} + 2s^{1.45} + 0.000067s^4 + 0.0023s^3 - 0.13s^2 - 0.4s$$

The roots of natural degree quasi characteristic polynomial inside the Riemann sheet then reveal instability, while roots lie outside the Riemann sheet then reveal the system's stability. In Fig. 9 all the roots are lying outside the Riemann sheet.

Robustness analysis:

The graphical investigation of the suggested controller for robustness can be establish in Fig. 10 For the determination of robustness utilize the equation (4.3), (4.4),(4.5). The presented controllers is demonstrated a smaller peak for nominal and 10% model mismatch cases.

V. CONCLUSION

This work uses a decomposed outer loop process model in series cascade control, constructed together with a fractional IMC filter, inverse response, and dead-time compensation. The inner loop and the first decomposed component of the outer loop are designed using the traditional integer order IMC controller. The outer loop controller is designed using a higher-order fractional IMC filter with an inverse and dead-time compensator. The outer loop controller has shown better performance, primarily in dead time behavior correction and inverse response. A few typical plant models from the literature have been used for the simulation work in order to emphasize the advantages of the proposed controller design. Employing the Riemann sheet principle, stability analysis has been performed. Sensitivity analysis was utilized as well to figure out the efficiency of the proposed controller. Finally, this work concludes

REFERENCES

- [1]. D.Seborg, F. E. Thomas, A. M. Ducan, Process Dynamics and Control, John Wiley and Sons, United state of America 2004.
- [2]. S. Uma, M. Chidambaram, A. Seshagiri Rao, C. K. Yoo, Chem. Eng. Sci. 2010, 65(3), 1065.
- [3]. O. Çakıroğlu, M. Güzelkaya, I. Eksin, Trans. Inst. Meas. Control 2015, 37(5), 623.
- [4]. P. R. Dasari, L. Alladi, A. Seshagiri Rao, C. Yoo, J. Process Control 2016, 45, 43.
- [5]. G. L. Raja, A. Ali, ISA Trans. 2021, 114, 191.
- [6]. M.A.Siddiqui, M. N. Anwar, S. H. Laskar, M. R. Mahboob, ISA Trans. 2021, 114, 331.
- [7]. G. Stephanopoulos, Chemical Process Control: An Introduction to Theory Practice, Prentice-Hall, 2015.
- [8]. V. M. Alfaro, R. Vilanova, J. Process Control 2013, 23(4), 453.
- [9]. B. Maâmar, M. Rachid, ISA Trans. 2014, 53(5), 1620.
- [10]. E. Yumuk, M. Güzelkaya, I. Eksin, ISA Trans. 2019, 91, 196.
- [11]. P. Lino, G. Maione, Ain Shams Eng. J. 2018, 51(4), 557.
- [12]. S. Karan, C. Dey, Asia Pac. J. Chem. Eng. 2021, 16(2), e2591.
- [13]. R. Ranganayakulu, A. Seshagiri Rao, G. Uday Bhaskar Babu, Int. J. Syst. Sci. 2020, 51(10), 1699.
- [14]. M. I. Kalim, A. Ali, IFAC Pap. Online 2020, 53(1), 195.
- [15]. Kaya, M. Nalbantoğlu, Electr. Eng. 2016, 98, 299.
- [16]. D. Mukherjee, G. L. Raja, P. Kundu, J. Control Autom. Electr. Syst. 2021, 32(1), 30.
- [17]. Nagarsheth S.H. and Sharma S.N. (2020). Control of non-minimum phase system with dead time: a fractional system view point. *International Journal of System Sciences*, 51(4), 1-24.
- [18]. Raja, G. L. and Ali A. (2021b). Enhanced tuning of Smith predictor-based series cascade control structure for integrating. *ISA Transactions*, 114, 191-205.
- [19]. Patel, B. Patel, Pragna Vachhrajani, H., Shah, D. and Sarvaia, A. (2019). Adaptive smith predictor controller for total intravenous anaesthesia automation. *Biomedical Engineering Letters*, 9, 127-144.
- [20]. Goodwin, G. C., Graebe, S. F. and Salgado, M. E., (2001). *Control Systems Design*, Prentice-Hall.
- [21]. Kaya, I. (2020). Integral-Proportional Derivative tuning for optimal closed loop responses to control integrating processes with inverse response, *Transactions of the Institute of Measurement and Control*, 42(16), 3123-3134.